Remote Sensing Hydrothermal Alteration Zones in the Marysvale Volcanic Field, Tushar Mountains, UT; an Intercomparison of Landsat 8 and ASTER Imagery.

Noah Christensen[1], Matthew Olson[2]

Utah Valley University (10851943@uvu.edu)[1], Department of Earth Science, Utah Valley University[2]

UTAH VALLEY UVU UNIVERSITY

Abstract

Understanding available resources is crucial for enhancing energy security, environmental sustainability, and economic growth. Traditional geologic mapping is characterized by time-intensive and high-cost fieldwork, but through multispectral and hyperspectral remotely sensed imagery it is possible to instantly map extensive areas using unique properties of minerals in the reflected spectral signature of the electromagnetic spectrum. This study explores an intercomparison of mineral mapping using Landsat 8, and ASTER in the Marysvale Volcanic Field, Utah. The satellites were chosen due to their varying number of spectral channels, spectral ranges, and spatial resolutions, allowing for a cross-analysis of their strengths, weaknesses, and overall capabilities. All analysis was conducted through open-source applications to promote accessibility in future research and reproducibility. Developing accurate and accessible mineral mapping tools may be the next step in strengthening our knowledge of resource availability, without the need for rigorous traditional mapping methods.

Background

The Marysvale volcanic field in Utah is one of the largest volcanic fields in the western United States, known for its uranium and alunite deposits. The igneous rocks found here were intruded ~32-20 million years ago, due to the subduction of the Farallon plate. The area continues to have episodic volcanism due to the extension of the Basin and Range.

Characteristic Minerals for Varying Types of Alteration

Propylitic alteration: chlorite, epidote, and sericite.
Phyllic alteration: muscovite, kaolinite, and sericite.
Argillic alteration: kaolinite, halloysite, and dickite.
Silicic alteration: quartz, silica, and chalcedony.
Advanced argillic alteration: pyrophyllite, diaspore, and kaolinite.
Potassic alteration: K-feldspar and biotite.
Sodic alteration: albite and nepheline.

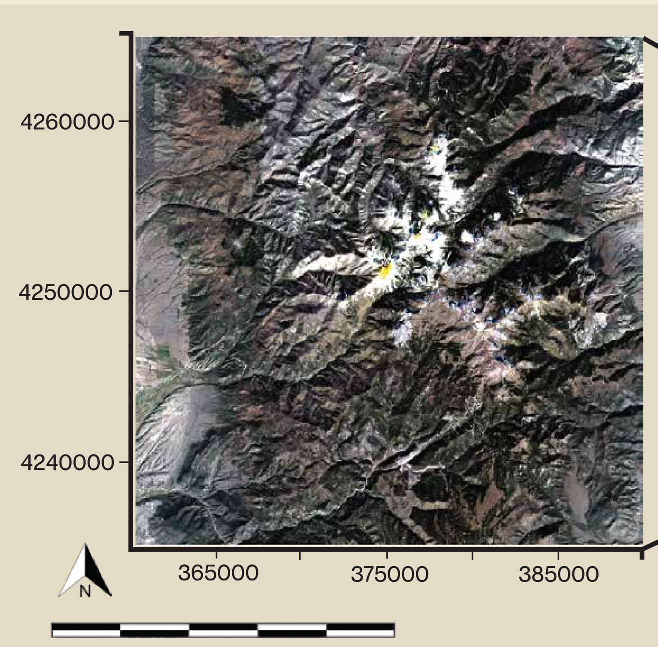

Figure 1a
RGB map of research extent using Landsat 8 imagery.
RGB created using Bands 4, 3, 2 respectively.
UTM zone 12N projection in WGS84.
Scales represent Easting (x-axis) and Northing (y-axis) in meters.

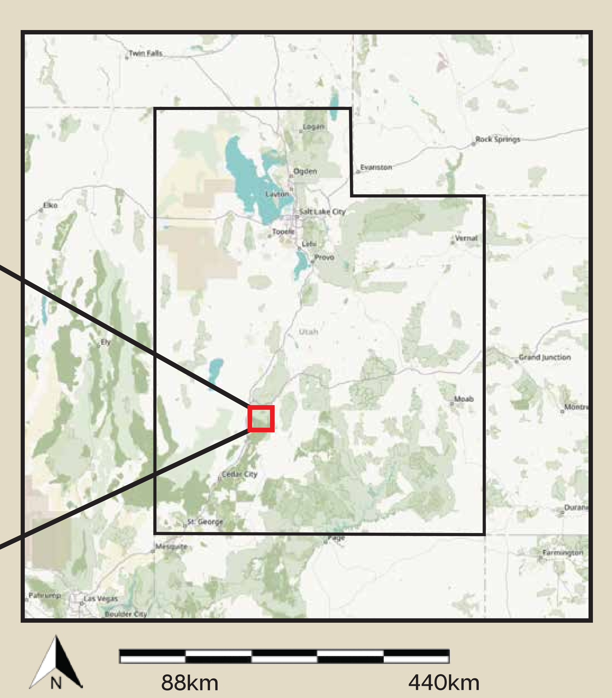

Figure 1b
Zoomed out view of Utah state border shown in black outline.
Research extent shown by red box.
Leaflet © OpenStreetMap contributors,
Tiles style by Humanitarian OpenStreetMap
Team hosted by OpenStreetMap France.

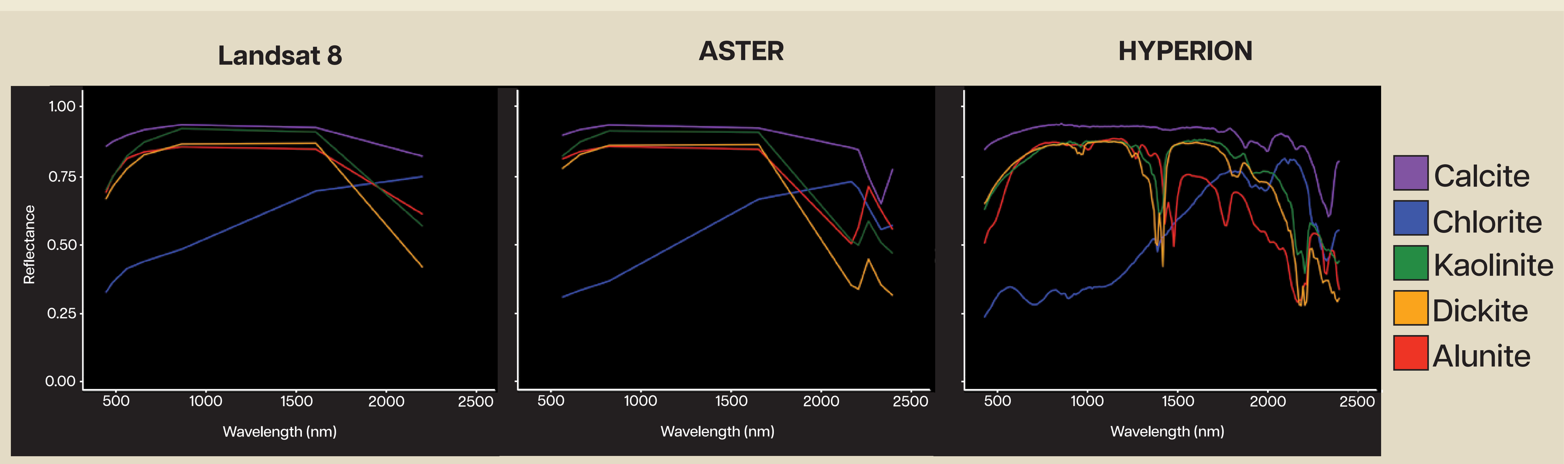

Figure 2
Spectral signatures for Calcite (purple), Chlorite (blue), Kaolinite (green), Dickite (orange), and Alunite (red) for Landsat 8 (left), ASTER (middle), and HYPERION (right).
Plotted using the USGS Spectral Library. Wavlength represented in nanometers on the x-axis and reflectance on x-axis.

Landsat

Sabins Ratio

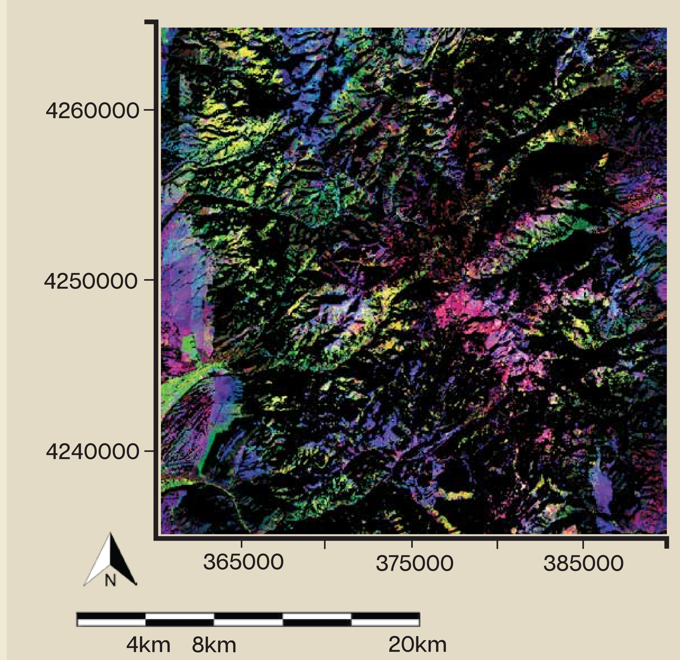

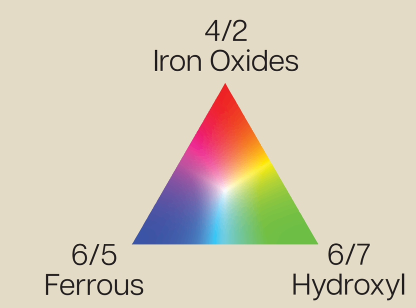

Hydrothermal alteration areas are represented by the association of green-pink or yellow zones.

Figure 3
Sabins Ratio map created using three bandmath equation of Landsat 8 imagery.
Red indicates Iron Oxide minerals, green indicated Hydroxyl minerals, and blue indicates Ferrous minerals.

Methods

Data collected from the USGS EarthExplorer

ASTER (L1B)

Landsat 8 (L2SP)

Transformed to Spectral Radiance
(Digital Number - 1) x gain value

Transform to Top of Atmosphere Reflectance
(π x Radiance x d^2)/(ESUN x cos(z))

CART supervised classifcation modeling to eliminate vegetated and snow covered areas from rasters

Applied bandmath equations for Sabins Ratio, hydrothermal alteration, and mineral maps

Applied manual thresholds to retain higher probablitiy pixels in mineral and hydrothermal alteration maps

Masking ASTER mineral maps by the hydrothermal alteration Map (Fig 4.)

d = Earth Sun Distance in Astronomical Units
ESUN = Mean Solar Exoatmospheric Irradiance of Each Band
z = Solar Zenith Angle

Gain value found in metadata

Collection ID for Landsat image: LC09_L2SP_038033_20231019_20231020_02_T1
Collection ID for ASTER image: AST_L1B_00310012005182513_20231130134446_13225

ASTER

Hydrothermal Alteration Map
(b4/b5)

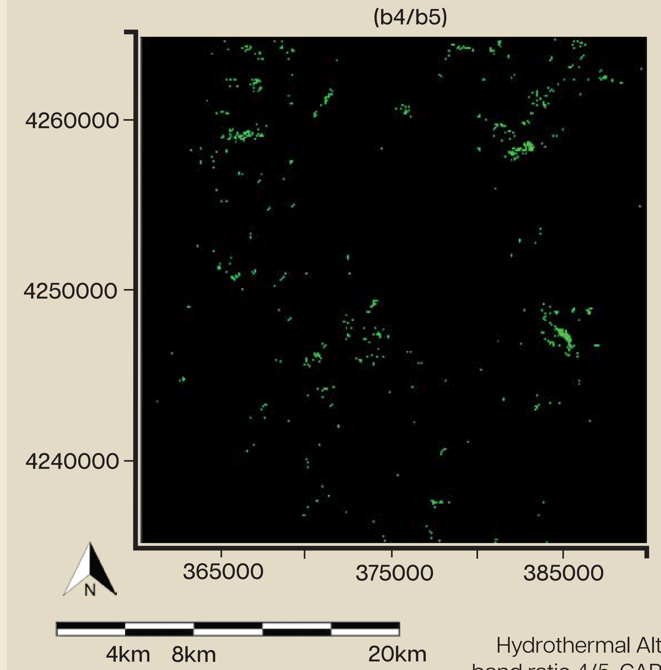

Minerals which are indicative of hydrothermal alteration have absorption features in the SWIR region. The band ratio enhances the spectral contrast of these features, making them more distinguishable.

Figure 4
Hydrothermal Alteratin Map created through the ASTER band ratio 4/5. CART modeling used to remove vegetation and snow cover. Manual threshold applied to remove noise and low probablity pixels.

Kaolinite, sericite, chlorite and epidote map
(b7+b9)/b8

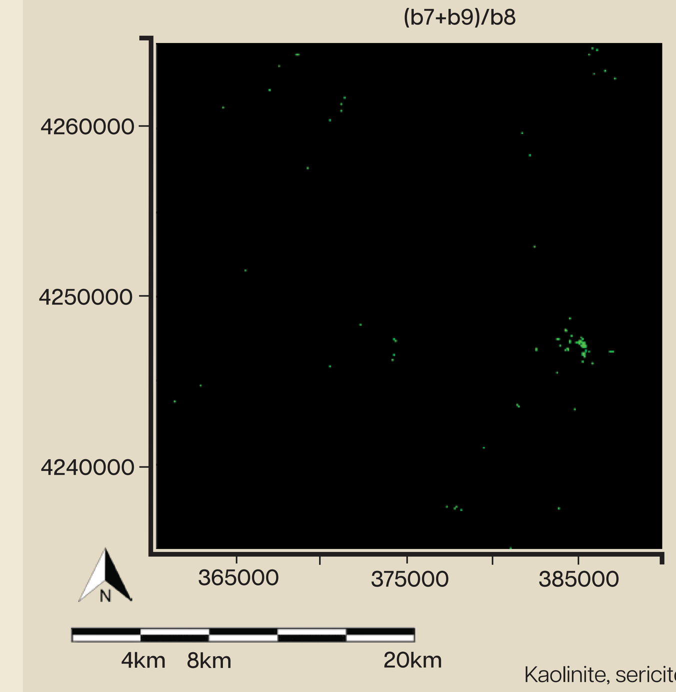

The South-East section was highlighted in the band math equation. These minerals occur in Phyllic or Argillic alteration.

Figure 5
Kaolinite, sericite, chlorite, and epidote map created through the ASTER band ratio (b7+b9)/b8
Masked by the Hydrothermal Alteration Map (Figure 4).

Host rock, Muscovite, Kaolinite (RGB)
Masked by Hydrothermal Alteration Map (Fig. 4)

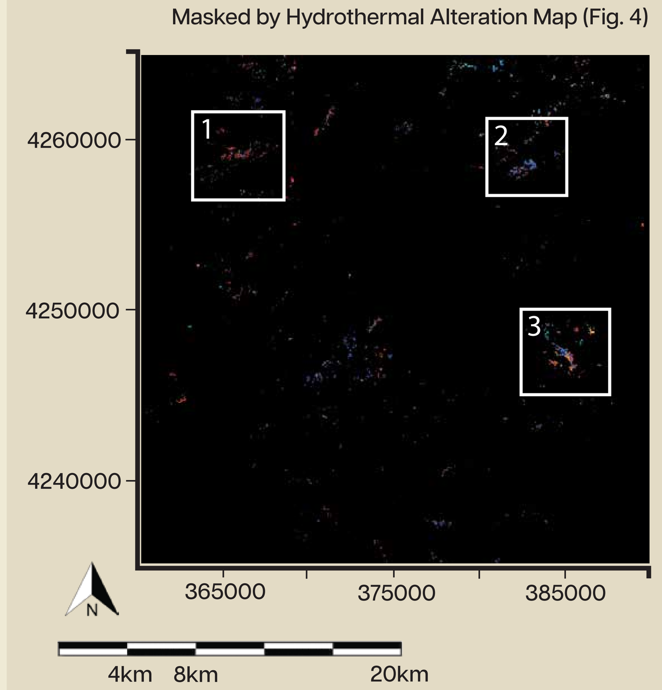

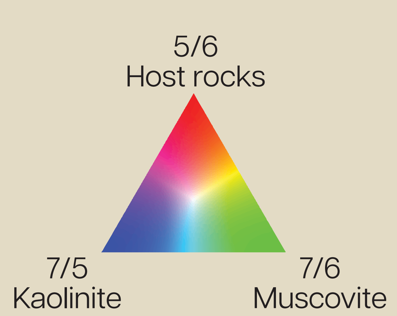

This map is an RGB composite showing Host rock, Muscovite, and Kaolinite respectiely. Masked by the Hydrothermal Alteration map (Figure 4.) Three zones of interest were highlighted and discussed in figure 6b.

The band ratios aim at highlighting varying absorbing minerals. Phengite may be present in red, muscovite and illite in green, and pyrophyllite, alunite, dickite, and kaolinite in blue. Red to tones are theoretically related to Aluminum poor area, and green to Aluminum rich.

Figure 6a
Host rock, Muscovite, and Kaolinite RGB. Mapped using ASTER bandmath.
Masked by the Hydrothermal Alteration Map (Figure 4).

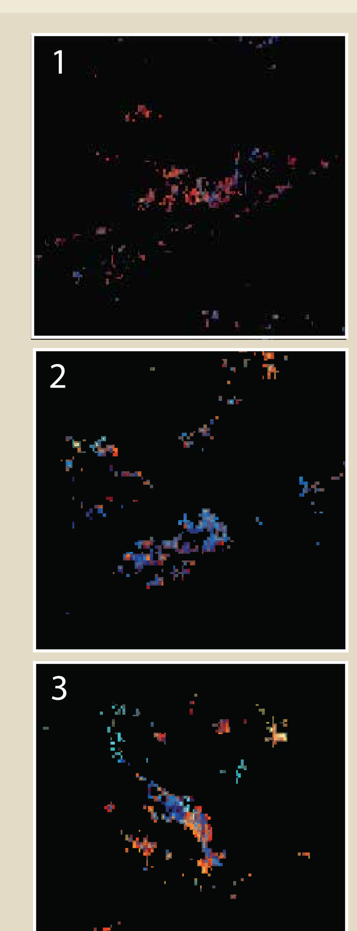

Area 1. contains mostly red pixels with a few blue areas throughout, this could be indication of no hydrothermal activity, or a phyllic alteration type.

Area 2. is prodiminately blue pixels, pointing towards an argillic alteration type.

Area 3. has both blue and red and blue areas, signaling either a Phyllic or Argillic alteration type

Figure 6b
Zoomed in zones of interest from Figure 6a. Three areas of interest highlighting potential hydrothermal activity and color indicative of alteration type.

Conclusion

The results of this study indicate that both Landsat 8 and ASTER imagery can provide valuable insights into hydrothermal alteration zones and their potential mineral assembleges. Landsat 8 it more limited in its application for mineral analysis due to the amount of spectral bands in the shortwave infrared and nearwave infrared; where minerals show their most diagnostic features. Landsat 8 did provide a similar delineation of large-scale alteration features and provided an overview of the distribution of alteration zones across the study area. However, ASTER, with its additional spectral bands, allowed for deeper delineation between minerals associated with hydrothermal alteration, contributing to a more in depth identification of alteration types. This finer level of detail is particularly valuable for understanding the geological processes and mineralogical composition of the Marysvale volcanics.

Continued research implimenting AVIRIS imagery and field validations will allow for mineral basis delineations, leading to a more accurate alteration zone type classification. AVIRIS being a hyperspectral sensor, allows for much more detail in mineral mapping, as well as finer area analysis due to the higher spatial resolution. Performing principle component analysis with AVIRIS can highlight specific spectral characteristics associated with minerals in a quick and efficient way.

Citations

Salem, S.M., El Sharkawi, M.A., El Alfy, Z. et al. The use of ASTER data and geochemical analyses for the exploration of gold at Samut area, South Eastern Desert of Egypt. Arab J Geosci 11, 541 (2018). https://doi.org/10.1007/s12517-018-3793-y

Osinowo, O. O., Gomy, A., & Isseini, M. (2021). Mapping hydrothermal alteration mineral deposits from Landsat 8 satellite data in Pala, Mayo Kebbi Region, Southwestern Chad. Scientific African, 11, e00687. https://doi.org/10.1016/j.sciaf.2020.e00687

Barnaby Whitson Rockwell. (2009). Comparison of ASTER- and AVIRIS-derived Mineral and Vegetation Maps of the White Horse Replacement Alunite Deposit and Surrounding Area, Marysvale Volcanic Field, Utah. Barnaby W. Rockwell.

Spectral Library | U.S. Geological Survey. (n.d.). Www.usgs.gov. https://www.usgs.gov/labs/spectroscopy-lab/science/spectral-library

USGS. (n.d.). EarthExplorer - Home. Earthexplorer.usgs.gov. https://earthexplorer.usgs.gov